

1  
2  
3  
4  
5  
6  
7  
8  
9  
10  
11  
12  
13  
14  
15  
16  
17  
18  
19  
20  
21  
22  
23  
24  
25  
26  
27  
28  
29  
30  
31

Received Date : 26-Dec-2016

Accepted Date : 24-Jan-2017

Article type : Articles

## **Estimating partial regulation in spatio-temporal models of community dynamics**

Running title: Spatio-temporal species interactions

James T. Thorson<sup>1\*</sup>, Stephan B. Munch<sup>2</sup>, Douglas P. Swain<sup>3</sup>

<sup>1</sup> Fisheries Resource Assessment and Monitoring Division, Northwest Fisheries Science Center, National Marine Fisheries Service, NOAA, Seattle, WA, USA;

<sup>2</sup> Fish Ecology Division, Southwest Fisheries Science Center, National Marine Fisheries Service, NOAA, 110 Schaffer Road, Santa Cruz, CA 95060;

<sup>3</sup> Gulf Fisheries Centre, Fisheries and Oceans Canada, P.O. Box 5030, Moncton, NB, Canada;

\* Corresponding author;

[James.Thorson@noaa.gov](mailto:James.Thorson@noaa.gov)

Telephone: 206-302-1772

Fax: 206-860-6792

### **Abstract**

Niche-based approaches to community analysis often involve estimating a matrix of pairwise interactions among species (the “community matrix”), but this task becomes infeasible using observational data as the number of modeled species increases. As an alternative, neutral theories achieve parsimony by assuming that species within a trophic level are exchangeable, but generally cannot incorporate stabilizing interactions even when they are evident in field data. Finally, both regulated (niche) and unregulated (neutral) approaches have rarely been

**This is the author manuscript accepted for publication and has undergone full peer review but has not been through the copyediting, typesetting, pagination and proofreading process, which may lead to differences between this version and the [Version of Record](#). Please cite this article as [doi: 10.1002/ecy.1760](https://doi.org/10.1002/ecy.1760)**

This article is protected by copyright. All rights reserved

32 fitted directly to survey data using spatio-temporal statistical methods. We therefore propose  
33 a spatio-temporal and model-based approach to estimate community dynamics that are  
34 partially regulated. Specifically, we start with a neutral spatio-temporal model where all  
35 species follow ecological drift, which precludes estimating pairwise interactions. We then  
36 add regulatory relations until model selection favors stopping, where the “rank” of the  
37 interaction matrix may range from zero to the number of species. A simulation experiment  
38 shows that model selection can accurately identify the rank of the interaction matrix, and that  
39 the identified spatio-temporal model can estimate the magnitude of species interactions. A  
40 forty-year case study for the Gulf of St. Lawrence marine community shows that recovering  
41 grey seals have an unregulated and negative relation with demersal fishes. We therefore  
42 conclude that partial regulation is a plausible approximation to community dynamics using  
43 field data, and hypothesize that estimating partial regulation will be expedient in future  
44 analyses of spatio-temporal community dynamics given limited field data. We conclude by  
45 recommending ongoing research to add explicit models for movement, so that meta-  
46 community theory can be confronted with data in a spatio-temporal statistical framework.

47 **Keywords:** neutral theory; community regulation; spatio-temporal model; Gulf of St.  
48 Lawrence; community matrix

## 49 **Introduction**

50 For at least 50 years, ecologists have conducted research on niche theory, which postulates  
51 that each species within a community occupies a unique ecological niche and that pairwise  
52 interactions arise from overlap in niche (Hutchinson 1957). Niche theory has encouraged  
53 ongoing research to measure the per-capita impact of one species on another for all pairs of  
54 species in a community or guild. In sharp contrast, several authors have introduced ‘neutral  
55 theories’ of ecology (Hubbell 2001, Harte 2011) in which species are viewed as exchangeable  
56 within a given trophic level or guild. Despite their clear differences, there is considerable  
57 empirical support for both niche and neutral theory. As with most binary distinctions in  
58 ecology (top-down v. bottom up, ratio-dependent v. prey-dependent, etc.), each theory may  
59 generate accurate and useful predictions of community dynamics for a particular temporal,  
60 spatial, taxonomic, and trophic scale. However, ecologists currently have few quantitative  
61 tools for combining insights from niche and neutral theories.

62 Inferring pairwise interactions remains one of the primary research goals in theoretical  
63 and applied ecology. However, species interactions are difficult to measure because the  
64 strength and sign of pairwise interactions depend on many circumstances, including (but not

65 limited to): the presence of additional species (Hixon and Carr 1997); environmental  
66 conditions (Morris 2003); and recent evolutionary history (Stegen et al. 2012). Manipulative  
67 experiments in micro- and mesocosms remain the gold-standard for inferring species  
68 interactions, but an increase in the number of species results in a factorial increase in the  
69 number of experimental treatments that must be conducted (Wootton and Emmerson 2005).  
70 Given these logistical difficulties, researchers have proposed two largely-independent  
71 approaches for predicting community dynamics: linear approximations using time series  
72 statistics, and neutral theories involving ecological drift.

73 Linear time-series approximations to community dynamics typically involve estimating  
74 the community matrix, defined as the matrix of impacts from increasing the abundance of one  
75 species on the per-capita productivity of every other species. The community matrix can be  
76 efficiently estimated using a multispecies extension of the Gompertz model for density  
77 dependence (Ives et al. 2003). Conveniently, this model also permits estimating the  
78 covariance of unexplained variation (termed “process errors” in the following). The  
79 estimated community matrix in this case represents a first-order Taylor series approximation  
80 to regulatory interactions, and Pfister (1995) gives support that this approach will estimate  
81 interactions with a sign and strength that matches manipulative experiments. Once the  
82 community matrix and process error covariance are estimated, results can be processed to  
83 yield a plethora of potential indicators of community stability, e.g., resilience or reactivity  
84 (Ives 1995, Neubert and Caswell 1997). Deyle et al. (2016) extend this framework to permit  
85 estimates of context-dependent species interactions but do not explicitly address the neutral-  
86 to-niche continuum.

87 By contrast, neutral theories typically postulate that all species (MacArthur and Wilson  
88 1967) or individuals (Hubbell 2001) have identical characteristics. Given this assumption,  
89 changes in broad-scale community patterns can then be explained via ecological drift, i.e., the  
90 random replacement of individuals or species within a local pool. This approach avoids  
91 estimating interactions for different species (because all species/individuals have identical  
92 interactions), and remaining parameters (fundamental biodiversity and immigration numbers)  
93 can be estimated from the species-abundance distribution (Etienne and Alonso 2005). Once  
94 parameters are estimated, species turn-over rates and species-abundance curves can be  
95 projected forward and backwards in time.

96 Both time-series and neutral theories for community structure and dynamics would  
97 benefit from including spatial variation explicitly. For example, Thorson et al. (2014)  
98 demonstrate that estimates of density dependence in time-series population models will be

99 biased whenever density varies spatially and density dependence acts locally, and that  
100 including spatial variation also improves precision by using spatial replication to increase  
101 statistical efficiency. A spatial analogue of time-series models for community dynamics may  
102 therefore result in improved accuracy and precision for predicting pairwise interactions and  
103 community stability. Spatial variation also underlies many important mechanisms for  
104 community stability (Chesson 2000), such that the estimate of spatio-temporal variation in  
105 productivity is useful in its own right. Similarly, neutral theories have generally included  
106 space explicitly, e.g., by including the density of individuals (Hubbell 2001) or energy (Harte  
107 2011) as model elements. However, research has underlined the importance of spatial  
108 variation in environmental conditions (Gilbert and Lechowicz 2004, Gilbert et al. 2006) or  
109 spatio-temporal variation in habitat suitability (Dornelas et al. 2006) to predictions arising  
110 from neutral theory. We therefore hypothesize that estimating spatial and spatio-temporal  
111 variation in productivity within neutral theory will in some cases improve estimates of  
112 community dynamics.

113 We therefore develop a spatio-temporal approach to estimating community dynamics,  
114 where data can be used to discriminate between neutral or highly regulated dynamics. In  
115 particular, we focus on determining the number of regulatory relations that are identifiable  
116 from a given community data set. To do so, we propose a new approach, which proceeds  
117 from the null hypothesis that all species follow identical, unregulated ecological drift (neutral  
118 dynamics) and successively adds axes of regulation until adding an additional regulatory  
119 relation is not parsimonious. This approach provides a continuum between estimating 0 and  
120  $P^2$  parameters for density dependence (approximating neutral and fully-regulated dynamics,  
121 respectively, where  $P$  is the number of species), and estimating fewer than  $P^2$  parameters is  
122 accomplished without zeroing out any single pairwise interaction. We then demonstrate the  
123 approach using a simulation experiment and a case study involving growth of grey seals  
124 impacting the fish community in the Gulf of St. Lawrence. Using these examples, we show  
125 that we can identify “partial regulation” (a combination of neutral and regulated components)  
126 in artificial and real-world data sets while accounting for spatio-temporal variation in  
127 productivity and density. By potentially estimating few than  $P^2$  parameters for the species  
128 interactions, we also hypothesize that our spatio-temporal approach will be computationally  
129 feasible for large communities.

## 130 **Methods**

131 Time series models for the dynamics of natural communities typically involve a nonlinear  
 132 function for growth of each population:

$$\mathbf{n}_{t+1} = f(\mathbf{n}_t) \circ \exp(\boldsymbol{\varepsilon}_{t+1}) \quad (1)$$

133 where  $\mathbf{n}_t$  is a vector of abundances for each of  $P$  species in time  $t$  (i.e.

134  $\mathbf{n}_t = \{n_{1,t}, n_{2,t}, \dots, n_{P,t}\}^T$ ),  $f(\mathbf{n}_t)$  is a potentially nonlinear, vector-valued function  
 135 representing inter- and intra-specific interactions for all species in the community, and we use  
 136  $\circ$  to indicate the Hadamard (elementwise) product of two vectors.  $\boldsymbol{\varepsilon}_t$  is a vector of random  
 137 effects that approximates unmodeled variation in community dynamics, including time-  
 138 dependence in  $f$  (which is assumed to be fixed in Eq. 1). Process errors are generally  
 139 assumed to follow some exchangeable process, e.g.:

$$\boldsymbol{\varepsilon}_t \sim \text{MVN}(\mathbf{0}, \boldsymbol{\Sigma}_{\text{process}}) \quad (2)$$

140 where  $\boldsymbol{\Sigma}_{\text{process}}$  is the covariance of process errors. We take the first-order Taylor's series  
 141 expansion of  $\mathbf{x}_t \equiv \ln(\mathbf{n}_t)$  around  $\bar{\mathbf{x}}_t$ , defined as the average observed value for  $\ln(\mathbf{n}_t)$  during  
 142 an interval  $T_{\min} \leq t \leq T_{\max}$ . This results in a linear approximation to dynamics:

$$\mathbf{x}_{t+1} = \boldsymbol{\alpha} + \mathbf{C}\mathbf{x}_t + \boldsymbol{\varepsilon}_{t+1} \quad (3)$$

143 where  $\mathbf{C}$  is a simple transformation of the community matrix such that a 1% increase in  
 144 species  $j$  results in a  $c_{i,j}$ % increase in productivity for species  $i$  (in other words:  $c_{i,j} =$   
 145  $\frac{\partial}{\partial \ln[n_j]} \ln [f(n_i)]$ ), average productivity is:

$$\boldsymbol{\alpha} = \ln[f(e^{\bar{\mathbf{x}}})] - \mathbf{C}\bar{\mathbf{x}} \quad (4)$$

146 and process errors  $\boldsymbol{\varepsilon}_t$  now accounts for both time-dependence in  $\mathbf{C}$  and  $\boldsymbol{\alpha}$ , as well as second-  
 147 and higher-order components of the Taylor-series approximation.

148 Using this approximation, community dynamics are stable as long as the modulus of all  
 149 eigenvalues of  $\mathbf{C}$  are between -1 and 1. In this case, community equilibrium is:

$$\mathbf{x}^* = (\mathbf{I} - \mathbf{C})^{-1}\boldsymbol{\alpha} \quad (5)$$

150 and it is relatively easy to calculate metrics of community stability including (1) the variance  
 151 around this equilibrium or (2) the reactivity of the stationary distribution (i.e., the ratio of the  
 152 expected distance from community state  $\mathbf{x}$  to equilibrium  $\mathbf{x}^*$ , given that  $\mathbf{x}$  is drawn from its  
 153 stationary distribution).

154 There are three potential problems with this formulation for community dynamics:

- 155 1. *Partial regulation*: Equilibrium properties of this model (Eq. 5) have previously been  
 156 derived only for the case of stable dynamics, i.e., when the eigenvalues of  $\mathbf{C}$  are inside the  
 157 unit circle. However, many reasonable ecological models contain non-hyperbolic  
 158 equilibria (for which the modulus of the dominant eigenvalue is equal to 1). In this case,

- 159 there is one or more axis that cannot be distinguished from following a random-walk  
160 process in log-densities.
- 161 2. *Veil of uncertainty*: Following the argument in Strong (1986), we suspect that many  
162 communities have regulation that is only distinguishable sporadically and for long time  
163 series (i.e., due to densities reaching extreme values, or due to density-dependent  
164 responses to infrequent environmental conditions). In these cases, many real-world data  
165 sets will not have any appearance of (or information about) the form of regulation that has  
166 permitted the community to persist long enough to generate the observed diversity of  
167 species. In these cases, we believe that it is pragmatic to begin with the assumption of no  
168 regulation (i.e.,  $\mathbf{C} = \mathbf{I}$ ), and then identify axes of regulation until there is no further  
169 information to identify regulation. This process may result in a stable community matrix  
170 (i.e.,  $\mathbf{C} - \mathbf{I}$  having rank  $P$ ), but may also result in an estimate of the community matrix  
171 with neutral stability.
- 172 3. *Curse of dimensionality*: The number of parameters in the community matrix  $\mathbf{C}$  increases  
173 as  $P^2$ . However, adding subsequent species to a community dynamics analysis often  
174 results in adding species with fewer and fewer observations. We therefore seek an  
175 approximation to  $\mathbf{C}$  that might have fewer parameters than  $P^2$ , but where model-selection  
176 tools can be used to identify the degree of dimension-reduction, and where model  
177 selection can potentially result in the unrestricted  $\mathbf{C}$  (with  $P^2$  degrees of freedom) being  
178 identified as parsimonious.

179 For these three different but interrelated reasons, we propose a procedure for estimating  
180 partial regulation in natural communities.

### 181 **Partial regulation, and its connection to neutral dynamics**

182 In the following, we develop a new parameterization for the community matrix. We begin  
183 with a re-parameterization of our linear approximation (Eq. 3):

$$\Delta \mathbf{x}_{t+1} = \boldsymbol{\alpha} + \mathbf{B} \mathbf{x}_t + \boldsymbol{\varepsilon}_{t+1} \quad (6)$$

184 such that  $\mathbf{B} = \mathbf{C} - \mathbf{I}$ , where abundance  $\mathbf{x}_{t=1}$  in the first year is estimated for each species. In  
185 particular, we seek a form of  $\mathbf{B}$  where one or more linear combinations of log-density for  
186 each species follows ecological drift (i.e.,  $\mathbf{B}$  has one or more eigenvalues equal to zero), and  
187 where the rank  $R$  of  $\mathbf{B}$  ( $0 \leq R \leq P$ ) contains information regarding the mix of neutral and  
188 regulated components to community dynamics. Specifically, a rank  $R$  for the interactions  
189 matrix  $\mathbf{B}$  implies that  $P - R$  linear combinations of log-density follow ecological drift. Given  
190 that  $\mathbf{B}$  has rank  $R$ , then  $\mathbf{B}$  has at most  $P^2 - (P - R)^2$  degrees of freedom. In particular, we

191 use a parameterization such that parameters  $\theta$  can be uniquely mapped onto  $\mathbf{B}$  (i.e.,  $g(\theta) \mapsto$   
192  $\mathbf{B}$ , where  $g$  is a differentiable function), and where we can place bounds on the non-zero  
193 eigenvalues. Appendix S1 proposes two functions for this task, where method #1 restricts  $\mathbf{B}$   
194 to have real-valued eigenvalues while method #2 allows both real and complex eigenvalues.  
195 However, exploratory analysis shows that restricting  $\mathbf{B}$  to have real-valued eigenvalues is  
196 more numerically stable for parameter estimation, so we use this version for subsequent case-  
197 study and simulation examples. Importantly, both methods allow the model to bridge  
198 between 0 and  $P^2$  parameters for density dependence, and both methods allow estimation of  
199 non-zero interactions for all pairs of species even when  $R < P$  (i.e.,  $b_{p,p^*} \neq 0$  for all species  
200  $p$  and  $p^*$  even when estimating fewer than  $P^2$  density-dependence parameters)

201 Having defined this model, we note that the case of  $R = 0$  results in  $\mathbf{B} = \mathbf{0}$ , such that  
202  $\Delta \mathbf{x}_{t+1} = \alpha + \epsilon_{t+1}$ . In this case, log-density for each species follows a random-walk process  
203 with drift  $\alpha$ , i.e., geometric growth rate for each species is normally distributed with mean  $\alpha$   
204 and covariance  $\Sigma_{\text{process}}$ . Random-walk dynamics represent a process where each population  
205 follows an exponential increases or decay on average but has stochastic variation around this  
206 level (termed “ecological drift”). Although this definition allows species-specific growth  
207 rates, we recover the standard definition of neutrality (e.g., as defined by Hubbell (2001)) if  
208  $\alpha_p$  is identical for all species. When  $\alpha = \mathbf{0}$  for each species, then the community follows  
209 ecological drift starting from initial abundance  $\mathbf{x}_{t=1}$ .

210 We hypothesize that ecological drift (i.e.,  $R = 0$ ) is a reasonable approximation to  
211 community dynamics over short time periods, where  $\alpha$  governs whether abundance for each  
212 individual species is expected to increase or decrease over short periods. However, long-term  
213 dynamics of this model are not biologically realistic when  $\mathbf{B} = \mathbf{0}$  and  $\alpha = \mathbf{0}$  because, in the  
214 limit as time goes to infinity, the expected population size for each species will go to infinity.  
215 This occurs because each species follows a random-walk process in log-space, such that  
216 extinction is impossible and the variance in log-space goes to infinity. When specifying  
217 neutral dynamics, the model can be estimated with as few as one freely-estimated parameter  
218 ( $\Sigma_{\text{process}} = \sigma^2 \mathbf{I}$ ). Longer term dynamics can also be stabilized by deriving a value of  $\alpha < \mathbf{0}$   
219 that results in finite asymptotic population sizes given the magnitude of process error.  
220 Presumably such a model could be parameterized to generate lognormal species-abundance  
221 curves, following a calculation similar to Engen and Lande (1996), although we do not  
222 pursue the idea here.

## 223 **Spatio-temporal community dynamics**

224 Previous research suggests that spatio-temporal models can provide more accurate and  
 225 precise estimates of single-species density dependence (Thorson et al. 2014). We therefore  
 226 estimate parameters using a spatio-temporal version of the community-dynamics model. This  
 227 involves replacing all scalar-valued variables with vectors representing density at each of  $S$   
 228 sites within a 2-dimensional spatial domain (Cressie and Wikle 2011). We specifically  
 229 replace the vector of log-abundance  $\mathbf{x}_t$  for each species in year  $t$  with a matrix  $\mathbf{X}_t$  with  
 230 dimension  $P$  by  $S$  representing log-density  $x_{t,p,s}$  in time  $t$  for species  $p$  at site  $s$ , replace  
 231 productivity  $\mathbf{a}$  with  $\mathbf{A}$  representing productivity  $a_{p,s}$  for species  $p$  at site  $s$ , and replace  
 232 process errors  $\boldsymbol{\varepsilon}_t$  with  $\mathbf{E}_t$  representing unexplained variation  $\varepsilon_{t,p,s}$ . The model therefore  
 233 becomes:

$$\mathbf{X}_{t+1} = \mathbf{A} + (\mathbf{I} + \mathbf{B})\mathbf{X}_t + \mathbf{E}_{t+1} \quad (7)$$

234 where the expectation of initial log-abundance for each species and site ( $x_{t=1,p,s}$ ) is estimated  
 235 as a fixed offset  $\beta_p$  from the productivity at that site. Specifically, we specify  $x_{t=1,p,s} =$   
 236  $a_{p,s} + \beta_p + \varepsilon_{t=1,p,s}$ , where the variance of initial log-abundance away from its expectation is  
 237 identical to the variance of process errors (future studies could explore more-complicated  
 238 specifications for initial conditions). We also specify a distribution for spatial variation in  
 239 productivity:

$$\text{vec}(\mathbf{A}) \sim \text{MVN}(\boldsymbol{\mu}_A, \mathbf{R}_{\text{spatial}} \otimes \boldsymbol{\Sigma}_A) \quad (8)$$

240 where  $\boldsymbol{\mu}_A$  is the median productivity across space,  $\boldsymbol{\Sigma}_A$  is a  $p$  by  $p$  diagonal matrix where each  
 241 diagonal element is the pointwise spatial variance  $\sigma_p^2$  for each species  $p$ , and  $\mathbf{R}_{\text{spatial}}$  is a  
 242 spatial correlation matrix. Spatial correlations are defined such that the pairwise correlation  
 243 between location  $s$  and  $s + h$  follows a Matérn function with smoothness of one:

$$\mathbf{R}_{\text{spatial}}(s, s + h) = \frac{1}{2^{\nu-1}\Gamma(\nu)} \times (\kappa|h|)^{\nu} \times K_{\nu}(\kappa|h|) \quad (9)$$

244 where  $\kappa$  is a parameter governing the distance  $h$  at which two locations are effective  
 245 uncorrelated,  $\nu$  is a smoothness parameter [fixed at 1.0; Simpson *et al.* (2012)] and  $K_{\nu}$  is the  
 246 Bessel function. Process errors  $\mathbf{E}_t$  are also defined spatially:

$$\text{vec}(\mathbf{E}_t) \sim \text{MVN}(\mathbf{0}, \mathbf{R}_{\text{spatial}} \otimes \boldsymbol{\Sigma}_E) \quad (10)$$

247 We use a reduced-rank approximation for covariance among species,  $\boldsymbol{\Sigma}_E = \mathbf{L}\mathbf{L}^T$ , such that  $\boldsymbol{\Sigma}_E$   
 248 has rank  $k$  and is calculated from a  $p$  by  $k$  matrix  $\mathbf{L}$  (Warton et al. 2015, Thorson et al. 2016).  
 249 In the following, however, we specify full rank for  $\boldsymbol{\Sigma}_E$  (i.e.,  $K = P$ ). This model makes three  
 250 important simplifying assumptions: (1) that interactions are constant over space and time  
 251 (i.e.,  $\mathbf{B}$  is not indexed by location or year), (2) that spatial variation in productivity is



252 statistically independent among species, and (3) that the decorrelation distance for each  
 253 species is identical (i.e.,  $\kappa$  does not vary among species). Each of these assumptions could be  
 254 relaxed in future research, but we do not explore them further here.

255 Parameters are estimated using sampling data, and we assume that sampling data are  
 256 proportional to local density for each species. We use the following observation model for  
 257 continuous-valued data (i.e., samples in units of biomass):

$$\begin{aligned}
 &P(C = c_p(i) | x_{t(i),p(i),s(i)}) && (11a) \\
 &= \begin{cases} \exp(-z_{p,2}\lambda_p(i)) & \text{if } C = 0 \\ \left(1 - \exp(-z_{p,2}\lambda_p(i))\right) \times \text{Lognormal}\left(C; \ln\left(\frac{\lambda_p(i)}{1 - \exp(-z_{p,2}\lambda_p(i))}\right), z_{p,1}^2\right) & \text{if } C > 0 \end{cases}
 \end{aligned}$$

258 where  $z_{p,1}$  is the standard deviation (in log-space) for non-zero samples, and  $z_{p,2}$  governs the  
 259 relationship between the probability of not encountering the species in a sample and the  
 260 predicted density for species  $p$ , such that probability of a zero sample ( $C=0$ ) is identical to a  
 261 Poisson distribution with intensity  $z_{p,2}\lambda_p(i)$  (i.e.,  $\Pr(C > 0)$  is described using a generalized  
 262 linear mixed model using a complementary log-log link). We use a lognormal distribution so  
 263 that future studies could interpret the magnitude of residual variation  $z_{p,1}^2$  relative to spatio-  
 264 temporal process errors ( $\Sigma_E$ ). Alternatively, if samples are count valued (i.e., have units  
 265 numbers) we use the Poisson distribution:

$$P(C = c_p(i) | x_{t(i),p(i),s(i)}) = \text{Poisson}(\lambda_p(i)) \quad (11b)$$

266 where in either case,  $\lambda_p(i) = \exp(x_{t(i),p(i),s(i)})$ , where  $x_{t(i),p(i),s(i)}$  is the estimated log-  
 267 density for the species, year, and site of the  $i^{\text{th}}$  observation. If sampling is proportional to  
 268 local density with detectability  $q_p$  for each species, and detectability is constant over time and  
 269 space but not perfect ( $q_p \neq 1$ ), then this will bias estimates of productivity ( $a_{p,s}$ ) and  
 270 absolute density ( $\mathbf{X}_t$ ) but will not otherwise affect estimates of interactions ( $\mathbf{B}$ ) or relative  
 271 differences in density across time and space for a single species ( $x_{t,p,s} / \sum_{t=1}^T \sum_{s=1}^S x_{t,p,s}$ ).

## 272 **Parameter estimation for spatio-temporal community dynamics**

273 While estimating parameters, we treat the parameters governing interactions ( $\Theta$ ), process  
 274 error covariance ( $\mathbf{L}$ ), the geostatistical range for correlations ( $\kappa$ ), average productivity for  
 275 each species ( $\mu_A$ ), the magnitude of spatial variation in productivity for each species ( $\sigma_p^2$ ), the  
 276 average offset of initial log-abundance from productivity for each species ( $\beta_p$ ), and  
 277 potentially the parameters governing the observation model if using catch-in-biomass data ( $\mathbf{z}$ )  
 278 as fixed effects. This set of parameters is arguably the minimum number required to account

279 for spatial variation (i.e., a Grinnelian niche) for each species, correlated responses to spatio-  
280 temporal variation, and the potential for species interactions. We treat as random the spatial  
281 variation in productivity ( $\mathbf{A}$ ), and the spatial variation in density for each species and year  
282 ( $\mathbf{X}_t$ ). We treat density as random, rather than process errors ( $\mathbf{E}_t$ ) because this results in a  
283 more separable specification for random effects without affecting the overall likelihood of  
284 fixed effects. This increased separability for random effects then leads to faster parameter  
285 estimation. Modeling random effects is a procedure for eliciting the expected covariation in  
286 data arising from a proposed set of fixed effects. Although fixed effects can generally be  
287 estimated for neutral models without recourse to numerical integration techniques (e.g.,  
288 Etienne and Alonso 2005), the increased complexity of our model required using numerical  
289 integration within a mixed-model statistical framework for estimating the small number of  
290 fixed effects. Despite our use of numerical integration for random effects representing  
291 density and spatial variation, the model involves a small number of free parameters relative to  
292 the amount of available data. Our model using full process-error rank and the observation  
293 model for counts (Eq. 11b) bridges between  $1 + 3.5P + 0.5P^2$  parameters (when dynamics  
294 are unregulated) and  $1 + 3.5P + 1.5P^2$  parameters (when dynamics are fully regulated). For  
295 biomass sampling data (Eq. 11a), our chosen configuration also involves an additional  $2P$   
296 parameters for the observation model.

297 To identify maximum likelihood estimates for fixed effects, we identify their values that  
298 maximize the marginal likelihood function when integrating across random effects. To do so,  
299 we use Template Model Builder, TMB (Kristensen 2014, Kristensen et al. 2016) called from  
300 within the R statistical environment (R Core Team 2015), and use the Microsoft R Open  
301 build for low-level parallelization of all computations (<https://mran.revolutionanalytics.com/>).  
302 For computational efficiency, we also use a stochastic partial differential equation  
303 approximation to all multivariate-normal distributions (i.e.,  $\mathbf{A}$  and  $\mathbf{E}_t$ ), and also approximate  
304 these function-valued variables as being piecewise-constant in the neighborhood of a small  
305 number of “knots”, where the number of knots is chosen as a balance of computational speed  
306 and precision (Lindgren et al. 2011, Thorson et al. 2014, 2015). Estimating parameters using  
307 Template Model Builder involves the following steps: (1) specify the joint log-likelihood of  
308 data and random effects; (2) given specified values of fixed effects, use TMB to identify  
309 values of random effects that maximize the joint log-likelihood; (3) given these values for  
310 fixed and random effects, use TMB to calculate the Laplace approximation to the marginal  
311 likelihood for fixed effects, and its gradient with respect to fixed effects (see e.g., Skaug and

312 Fournier 2006); and (4) use the marginal likelihood and its gradients within a nonlinear  
313 minimizer in R to identify maximum likelihood estimates for fixed effects.

314 We identify model convergence by confirming that the absolute-value of the final  
315 gradient of the marginal likelihood with respect to fixed effects is  $<0.01$  for all parameters,  
316 and that the Hessian matrix is positive definite. After identifying maximum likelihood  
317 estimates for fixed effects and confirming convergence, TMB then identifies empirical Bayes  
318 estimates of random effects, and uses a generalized delta method to calculate standard error  
319 estimates for all fixed and random effects. An R package MIST to apply this Multispecies  
320 Interactions Spatio-Temporal model to new data sets is available on the first author's GitHub  
321 page (<https://github.com/James-Thorson/MIST>), and we used v1.1.0 (DOI  
322 10.5281/zenodo.260143). By using maximum likelihood methods for parameter estimation,  
323 we allow hypothesis testing and probabilistic comparisons of neutral and niche approaches,  
324 as advocated by McGill et al. (2006).

### 325 **Simulation experiment**

326 We conducted a simulation experiment to explore the statistical properties of our proposed  
327 model. Specifically we seek to determine:

- 328 1. whether we can accurately estimate the interaction matrix ( $\mathbf{B}$ ); and
- 329 2. whether model selection tools can accurately identify the number of regulatory  
330 relationships ( $R$ ), where this number can range from zero (i.e.,  $\mathbf{B}=\mathbf{0}$ ) to  $P$  (i.e.,  $\mathbf{B}$  is  
331 estimated with the restriction that its eigenvalues have range between  $-1$  and  $1$ ).

332 To conduct this experiment, we simulated 50 replicated data sets, where each data set  
333 involves dynamics for four species over 40 years. Dynamics occur at 25 sites that are  
334 randomly distributed following a 2-dimensional uniform distribution within a square domain,  
335 where each site is sampled in numbers twice per year (2,000 samples total per species). We  
336 simulated data using Eq. 7-10 and 11b, where  $\mu_A = 2.0$ ,  $\sigma_{\text{spatial}} = 0.01$ ,  $\Sigma_E = 0.05\mathbf{I}$ , where  
337  $\mathbf{R}_{\text{spatial}}$  is specified such that correlations drop to 10% at 20% of the length of an edge of the  
338 square spatial domain. We specified the interaction matrix:

$$\mathbf{B} = \begin{pmatrix} -0.4 & -0.4 & -0.1 & -0.05 \\ -0.4 & -0.4 & -0.1 & -0.05 \\ -0.1 & -0.05 & -0.3 & -0.3 \\ -0.1 & -0.05 & -0.3 & -0.3 \end{pmatrix} \quad (12)$$

339 i.e., where  $\mathbf{B}$  is composed of two species modules (Holt 1997), where species 1 and 2 are the  
340 first competitive module, and species 3 and 4 are the second competitive module. We also  
341 included weak competition among modules (such that all species have non-zero interactions),  
342 but where species 1 and 3 have stronger among-module competition than species 2 and 4

343 (such that all species have a unique set of interactions). Given this structure, community  
344 dynamics has two regulated and two unregulated components, i.e.,  $\mathbf{B}$  is within the family of  
345 matrices generated by  $R = 2$  (which has 12 degrees of freedom). We also compare results  
346 against a null model wherein  $\mathbf{B}$  is estimated as a diagonal matrix with independent parameters  
347 along the diagonal and process errors are also independent ( $\mathbf{\Sigma}_E$  is diagonal). This null model  
348 includes single-species density dependence in place of community-level regulation, and  
349 illustrates the magnitude of error arising from ignoring community interactions. Finally, we  
350 conduct a sensitivity analysis illustrating the effect of less-informative data. To do so, we  
351 conduct another simulation experiment that is identical except that initial log-abundance is  
352 decreased to  $\mu_A = 1.0$ . In both simulation experiments, we record the proportion of  
353 simulation replicates that result in non-convergence, and restrict results to converged models.

### 354 **Case study application**

355 To demonstrate this method, we use data for four species (Atlantic cod, thorny skate, white  
356 hake, and grey seal) in the Gulf of St. Lawrence from 1971 to 2012, which we previously  
357 published by Swain et al. (2015). This time series spans two (thorny skate) to four (white  
358 hake) generations at historical levels of natural mortality and age at maturation. Data for  
359 Atlantic cod, thorny skate, and white hake are obtained from a bottom trawl survey of fishes,  
360 and represent samples of biomass divided by area-swept by the bottom trawl (termed “catch-  
361 per-unit-effort”, CPUE, analyzed using Eq. 11a). Sampling follows a simple random design  
362 involving 63-231 samples per year (5,588 samples total), and for computational efficiency we  
363 assign each sampling location to the nearest of 100 uniformly distributed “knots” such that  
364 we estimate density at each of 100 knots ( $S = 100$ ) and spatial variation occurring at fine  
365 scales is attributed to residual variation ( $z_{p,1}^2$  in Eq. 11a). Data for grey seal are estimates of  
366 seal density obtained from analysis of seal tag sightings during this period. The data set  
367 therefore contains a mix of survey observations and model output. The data set has  
368 previously been analyzed by Swain et al. (2015), and it is not feasible to simultaneously  
369 estimate spatio-temporal community dynamics and reconstruct seal densities from raw tag-  
370 resighting data. However, the joint analysis of survey data as a Poisson process and tag-  
371 resighting data as a Markovian movement process would be an interesting topic for future  
372 research.

## 373 **Results**

### 374 **Simulation experiment**

375 We first explore results from our simulation experiment, where we simulate dynamics for  
376 four species with two regulated and two unregulated components (i.e., true  $R = 2$ ). In this  
377 case, model selection identifies a model with 2 regulated relationships in almost all  
378 simulation replicates, with 3 and 4 relations identified in a small proportion, and independent  
379 dynamics are never identified (Fig. 1 top panel). The model with 2 regulated relations  
380 converges in almost all simulation replicates (2%), although the model with independent  
381 dynamics is slightly more stable numerically (0% nonconvergence). Models with 2 or more  
382 regulated relations are able to improve predictions of density relative to either independent  
383 dynamics, or a model with only one regulatory relation (Fig. 1 bottom panel). Visualizing  
384 estimates of the interaction matrix ( $\mathbf{C} = \mathbf{B} + \mathbf{I}$ ) shows that the model generates essentially  
385 unbiased estimates of both within-module competition (e.g., species 1 and 2) and among-  
386 module competition (e.g., species 1 and 3, Fig. 2). Sensitivity analyses show that decreased  
387 sample sizes for sampling result in increased rates of non-convergence and degraded ability  
388 to identify the rank of the interaction matrix, but maintains approximately unbiased estimates  
389 of species interactions (Appendix S2, Fig. S1-S2). We therefore conclude that the model is  
390 able to accurately identify instances of partial regulation, e.g., to evaluate the strength of  
391 evidence in favor of neutral or niche-based approaches to community regulation, but that  
392 estimating full regulation ( $R = 4$ ) does not substantially degrade performance when  
393 estimating local density.

#### 394 **Case study: Gulf of St. Lawrence community dynamics**

395 Model selection from our case study identifies the model with three regulatory relationships  
396 as being parsimonious, thus identifying strongest evidence for partially regulated dynamics in  
397 this community. The estimated interaction matrix (Table 1) shows a strong, negative impact  
398 of grey seals on thorny skate, and a weak negative relation of grey seals on Atlantic cod  
399 (where the former is statistically significant using a 2-sided Wald test;  $-0.213$ ,  $SE=0.078$ ,  
400  $p < 0.01$ ). By contrast, Atlantic cod and white hake both have significant, positive impacts  
401 with thorny skate. The eigen-decomposition of this interaction matrix (Fig. 3) shows that the  
402 unregulated component of community dynamics is associated with the negative relation  
403 between grey seals and all fish species (top-left panel). Other relations have weak regulation  
404 (i.e., eigenvalues different from 1.0).

405 Inspecting density maps for each species (Fig. 4) shows that thorny skate has gone from  
406 being ubiquitous to having low density everywhere except in deeper water along the north-  
407 eastern seaward boundary. In contrast, grey seal has shown a marked increase in density in

408 shallower waters, particularly near the western coast of Prince Edward Island. By contrast,  
409 Atlantic cod showed an initial increase and subsequent decrease in density. Cod distribution  
410 shifted toward the central Magdalen Shallows during the increase and out of it during the  
411 decrease. In recent years, cod densities have decreased the most off the west of Prince  
412 Edward Island, the region where the increase in grey seal density has been most marked.  
413 White hake were initially distributed in warm deeper water along the north-eastern seaward  
414 boundary and in warm shallow inshore waters. Their density initially increased slightly in  
415 these areas and then declined. This decline was most severe in inshore areas, where white  
416 hake are now very rare. The estimated magnitude of process errors ( $\Sigma_{\text{process}} = \mathbf{L}\mathbf{L}^T$ ; Fig. 5)  
417 shows that Atlantic cod has the highest residual variation in density (a log-standard deviation  
418 of 0.22), while other species have lower residual variation (log-standard deviation of <0.20).  
419 Residual correlations are generally positive, and are stronger among the three fish species  
420 than between fishes and grey seals. This implies that processes in addition to pairwise  
421 interactions (e.g., environmental conditions) may cause synchronous variation in productivity  
422 for these fishes.

## 423 **Discussion**

424 In this paper, we have hypothesized that short-term dynamics for ecological communities will  
425 involve a mixture of regulated and unregulated components, and that the associated  
426 community matrix will be parsimonious in some cases. We then demonstrated a model for  
427 spatio-temporal community dynamics that uses model selection to identify regulation along a  
428 continuum ranging from neutral dynamics (where every species follows unregulated  
429 ecological drift) to stable dynamics (where the full community matrix of pairwise interactions  
430 is estimated). A simulation experiment confirms (1) that model selection is able to accurately  
431 identify the number of regulatory relationships given sufficient data, (2) that lack of  
432 convergence is associated with insufficient data to identify the number of regulatory  
433 relations, and (3) that models are generally able to estimate pairwise interactions. A case  
434 study illustrates our proposed approach for a trophically-linked community involving a  
435 recovering top predator (grey seals). Previous spatio-temporal models for ecological  
436 communities have generally involved a factor-analysis approach (Warton et al. 2015,  
437 Thorson et al. 2016), where dynamics for  $P$  species is approximated using  $R$  spatio-temporal  
438 factors ( $0 \leq R \leq P$ ). We have replaced this phenomenological description of spatio-  
439 temporal dynamics with a model that explicitly estimates significant pairwise interactions,  
440 but have retained both (1) the ability to estimate correlations in spatio-temporal dynamics

441 among species, and (2) the likely improvement in statistical efficiency from using spatial  
442 replication to estimate interactions.

443 We propose this approach to remedy issues in previous neutral and time-series  
444 approaches to community dynamics. In particular, time-series approaches require estimating  
445 pairwise interactions that increase as the square of the number of species, and this will likely  
446 not be parsimonious (or even identifiable) for large communities. Similarly, neutral models  
447 have important limitations, *inter alia*, previous criticism for failing to capture spatial variation  
448 (Gilbert and Lechowicz 2004, Gilbert et al. 2006) or spatio-temporal variation in habitat  
449 suitability for individual species (Dornelas et al. 2006). By contrast, our approach can be  
450 interpreted as a short-term approximation to neutral spatio-temporal dynamics when there are  
451 no regulatory relations ( $R = 0$ , such that  $\mathbf{B} = \mathbf{0}$ ) and no drift ( $\mathbf{A} = \mathbf{0}$ ). In this limiting case,  
452 our approach can be reduced to two parameters: the characteristic spatial scale, and the  
453 magnitude of spatio-temporal variation. The approach can then be expanded to include  
454 correlated responses to spatio-temporal variation, thereby accounting for similar responses to  
455 environmental conditions. Although we use numerical integration (rather than analytical  
456 integration as has been used previously to describe neutral dynamics, e.g., Etienne and  
457 Alonso (2005)), we argue that our approach bridges low- and high-dimensional applications.

458 Previous authors have noted that neutral theory is likely not a suitable approximation to  
459 community dynamics for species at different trophic levels (Hubbell 2001), for which the  
460 assumptions of identical per-capita impacts is particularly unlikely. By contrast, our study  
461 has shown that partially regulated community dynamics is occurring across two trophic levels  
462 in the Gulf of St. Lawrence. Specifically, the increase in predators (grey seals) is offset by a  
463 decrease in three prey species (fishes), while other axes of community dynamics are generally  
464 regulated. We acknowledge that this unregulated component of community dynamics will  
465 probably experience regulation in the future (i.e., the log-density of seals cannot follow a  
466 random-walk process forever). However, our model identifies that interactions between grey  
467 seals and fishes cannot be distinguished from unregulated dynamics during the past forty  
468 years.

469 Estimates of species interactions from this model agree well with the results of more  
470 detailed process-oriented studies for the Gulf of St. Lawrence marine community. The model  
471 estimates that grey seal abundance has followed a density-independent exponential increase.  
472 This is consistent with grey seal population studies which estimate a roughly exponential  
473 increase in grey seal abundance in Atlantic Canada over the past 55 years (Hammill et al.  
474 2014a). Despite a 50-fold increase in abundance, there is little evidence for a decline in

475 productivity over this period. Increasing seal population size was negatively associated with  
476 densities of all three fish species. These three species are (or have been) important prey of  
477 grey seals in the Gulf of St. Lawrence (Benoit and Bowen 1990, Hammill et al. 2014b). Their  
478 on-going declines, despite currently negligible fishing mortality, are the consequence of large  
479 increases in natural mortality, which appear to reflect increased predation by grey seals  
480 (Swain and Benoit 2015). The negative impact of seals is estimated to be strongest for thorny  
481 skate. Because of their slow life history (e.g., late maturation), thorny skate are expected *a*  
482 *priori* to be most vulnerable to increasing predation rates.

483 Importantly, our approach is low-dimensional relative to whole-of-ecosystem models that  
484 are frequently used for marine communities (Christensen and Walters 2004, Fulton et al.  
485 2011). An alternative low-dimensional approach to community modelling involves pre-  
486 specifying community modules (e.g., trophic or competitive structures), where species from  
487 different modules have weak or nonexistent interactions. However, small changes in the  
488 specification of food webs can result in large differences in community properties (Abrams  
489 1993). We therefore argue that the linear approximation to nonlinear dynamics (projecting  
490 Eq. 1 onto the space spanned by Eq. 3) remains a suitable approximation to short-term  
491 community dynamics (Ives et al. 2003), without requiring *a priori* specification of  
492 community interactions. Researchers have previously used model selection to exclude  
493 interactions that were not significantly different from zero (e.g., Hampton et al. 2006).  
494 However, we show that we can reduce the number of estimated parameters even without  
495 “zeroing-out” any pairwise interactions. In our case, we eliminate parameters by specifying  
496 that some axes of the community are unregulated, so that dynamics of these axes correspond  
497 to a random-walk process. This random-walk approximation for some axes of community  
498 dynamics appears to be a useful approximation over short time scales (e.g., when analyzing a  
499 small number of generations for some components of the community).

500 Finally, we note that our model does not explicitly account for individual movement.  
501 Modelling movement is important to ongoing research regarding spatially explicit neutral  
502 models (Etienne and Rosindell 2011), and is also central to “mass effects” and “patch  
503 dynamics” models for meta-communities (Shoemaker and Melbourne 2016). Furthermore,  
504 movement in search of preferred habitats often modifies predicted outcomes from pairwise  
505 competitive interactions (Morris 2003). Future research can explore incorporating advective-  
506 diffusive movement within multispecies spatio-temporal models (Thorson et al. In press,  
507 Hooten and Wikle 2010), but previous approaches are computation-intensive and would  
508 likely inhibit simulation testing. We therefore encourage further development of approximate



509 or exact solutions to advective-diffusive movement within spatio-temporal models of  
510 community dynamics. In particular, mixed-effects models show great promise in providing a  
511 general approximation to the statistical mechanics that also underlies theory for neutral  
512 models.

### 513 **Acknowledgments**

514 We thank Eric Ward and Mark Scheuerell for discussions regarding community dynamics,  
515 and Mark Scheuerell, Jim Hastie, Michelle McClure, and two anonymous reviewers for  
516 comments on an earlier draft.

517

### 518 **Literature Citations**

519 Abrams, P. A. 1993. Effect of increased productivity on the abundances of trophic levels.

520 *American Naturalist*:351–371.

521 Benoit, D., and W. D. Bowen. 1990. Seasonal and geographic variation in the diet of grey

522 seals (*Halichoerus grypus*) in eastern Canada. *Population biology of sealworm*:215–

523 226.

524 Chesson, P. 2000. Mechanisms of Maintenance of Species Diversity. *Annual Review of*

525 *Ecology and Systematics* 31:343–366.

526 Christensen, V., and C. J. Walters. 2004. Ecopath with Ecosim: methods, capabilities and

527 limitations. *Ecological Modelling* 172:109–139.

528 Cressie, N., and C. K. Wikle. 2011. *Statistics for spatio-temporal data*. John Wiley & Sons,

529 Hoboken, New Jersey.

530 Deyle, E. R., R. M. May, S. B. Munch, and G. Sugihara. 2016. Tracking and forecasting

531 ecosystem interactions in real time. *Proc. R. Soc. B* 283:20152258.

532 Dornelas, M., S. R. Connolly, and T. P. Hughes. 2006. Coral reef diversity refutes the neutral

533 theory of biodiversity. *Nature* 440:80–82.

534 Engen, S., and R. Lande. 1996. Population dynamic models generating the lognormal species

535 abundance distribution. *Mathematical biosciences* 132:169–183.

536 Etienne, R. S., and D. Alonso. 2005. A dispersal-limited sampling theory for species and

537 alleles. *Ecology Letters* 8:1147–1156.

538 Etienne, R. S., and J. Rosindell. 2011. The Spatial Limitations of Current Neutral Models of

539 Biodiversity. *PLOS ONE* 6:e14717.

540 Fulton, E. A., J. S. Link, I. C. Kaplan, M. Savina-Rolland, P. Johnson, C. Ainsworth, P.

541 Horne, R. Gorton, R. J. Gamble, A. D. M. Smith, and others. 2011. Lessons in

542 modelling and management of marine ecosystems: the Atlantis experience. *Fish and*  
543 *Fisheries*.

544 Gilbert, B., W. F. Laurance, E. G. Leigh Jr, and H. E. Nascimento. 2006. Can Neutral Theory  
545 Predict the Responses of Amazonian Tree Communities to Forest Fragmentation?\*.  
546 *The American Naturalist* 168:304–317.

547 Gilbert, B., and M. J. Lechowicz. 2004. Neutrality, niches, and dispersal in a temperate forest  
548 understory. *Proceedings of the National Academy of Sciences of the United States of*  
549 *America* 101:7651–7656.

550 Hammill, M. O., C. E. den Heyer, and W. D. Bowen. 2014a. Grey seal population trends in  
551 Canadian waters, 1960-2014. *Fisheries and Oceans Canada, Science*.

552 Hammill, M. O., G. B. Stenson, D. P. Swain, and H. P. Benoît. 2014b. Feeding by grey seals  
553 on endangered stocks of Atlantic cod and white hake. *ICES Journal of Marine*  
554 *Science: Journal du Conseil:fsu123*.

555 Hampton, S. E., M. D. Scheuerell, and D. E. Schindler. 2006. Coalescence in the Lake  
556 Washington story: Interaction strengths in a planktonic food web. *Limnology and*  
557 *Oceanography* 51:2042–2051.

558 Harte, J. 2011. *Maximum entropy and ecology: a theory of abundance, distribution, and*  
559 *energetics*. Oxford University Press, Oxford, UK.

560 Hixon, M. A., and M. H. Carr. 1997. Synergistic predation, density dependence, and  
561 population regulation in marine fish. *Science* 277:946.

562 Holt, R. D. 1997. Community modules. Pages 333–349 *Multitrophic interactions in terrestrial*  
563 *ecosystems, 36th Symposium of the British Ecological Society*. Blackwell Science  
564 Oxford.

565 Hooten, M. B., and C. K. Wikle. 2010. *Statistical Agent-Based Models for Discrete Spatio-*  
566 *Temporal Systems*. *Journal of the American Statistical Association* 105:236–248.

567 Hubbell, S. P. 2001. *The unified neutral theory of biodiversity and biogeography (MPB-32)*.  
568 Princeton University Press.

569 Hutchinson, G. E. 1957. Population studies-animal ecology and demography-concluding  
570 remarks. Pages 415–427 *Cold Spring Harbor Symposia on Quantitative Biology*.  
571 COLD SPRING HARBOR LAB PRESS 1 BUNGTOWN RD, PLAINVIEW, NY  
572 11724.

573 Ives, A. R. 1995. Measuring resilience in stochastic systems. *Ecological Monographs:217–*  
574 *233*.

575 Ives, A. R., B. Dennis, K. L. Cottingham, and S. R. Carpenter. 2003. Estimating community  
576 stability and ecological interactions from time-series data. *Ecological monographs*  
577 73:301–330.

578 Kristensen, K. 2014. TMB: General random effect model builder tool inspired by ADMB.  
579 Kristensen, K., A. Nielsen, C. W. Berg, H. Skaug, and B. M. Bell. 2016. TMB: Automatic  
580 Differentiation and Laplace Approximation. *Journal of Statistical Software* 70:1–21.

581 Lindgren, F., H. Rue, and J. Lindström. 2011. An explicit link between Gaussian fields and  
582 Gaussian Markov random fields: the stochastic partial differential equation approach.  
583 *Journal of the Royal Statistical Society: Series B (Statistical Methodology)* 73:423–  
584 498.

585 MacArthur, R. H., and E. O. Wilson. 1967. *The Theory of Island Biogeography*. Princeton  
586 University Press.

587 McGill, B. J., B. A. Maurer, and M. D. Weiser. 2006. Empirical evaluation of neutral theory.  
588 *Ecology* 87:1411–1423.

589 Morris, D. W. 2003. Toward an Ecological Synthesis: A Case for Habitat Selection.  
590 *Oecologia* 136:1–13.

591 Neubert, M. G., and H. Caswell. 1997. Alternatives to resilience for measuring the responses  
592 of ecological systems to perturbations. *Ecology* 78:653–665.

593 Pfister, C. A. 1995. Estimating Competition Coefficients from Census Data: A Test with  
594 Field Manipulations of Tidepool Fishes. *The American Naturalist* 146:271–291.

595 R Core Team. 2015. *R: A Language and Environment for Statistical Computing*. R  
596 Foundation for Statistical Computing, Vienna, Austria.

597 Shoemaker, L. G., and B. A. Melbourne. 2016. Linking metacommunity paradigms to spatial  
598 coexistence mechanisms. *Ecology* 97:2436–2446.

599 Simpson, D., F. Lindgren, and H. Rue. 2012. In order to make spatial statistics  
600 computationally feasible, we need to forget about the covariance function.  
601 *Environmetrics* 23:65–74.

602 Skaug, H., and D. Fournier. 2006. Automatic approximation of the marginal likelihood in  
603 non-Gaussian hierarchical models. *Computational Statistics & Data Analysis* 51:699–  
604 709.

605 Stegen, J. C., B. J. Enquist, and R. Ferrière. 2012. Eco-Evolutionary Community Dynamics:  
606 Covariation between Diversity and Invasibility across Temperature Gradients\*. *The*  
607 *American Naturalist* 180:E110–E126.

- 608 Strong, D. R. 1986. Density-vague population change. *Trends in Ecology & Evolution* 1:39–  
609 42.
- 610 Swain, D. P., and H. P. Benoît. 2015. Extreme increases in natural mortality prevent recovery  
611 of collapsed fish populations in a Northwest Atlantic ecosystem. *Marine Ecology*  
612 *Progress Series* 519:165–182.
- 613 Swain, D. P., H. P. Benoît, and M. O. Hammill. 2015. Spatial distribution of fishes in a  
614 Northwest Atlantic ecosystem in relation to risk of predation by a marine mammal.  
615 *Journal of Animal Ecology* 84:1286–1298.
- 616 Thorson, J. T., J. N. Ianelli, E. A. Larsen, L. Ries, M. D. Scheuerell, C. Szuwalski, and E. F.  
617 Zipkin. 2016. Joint dynamic species distribution models: a tool for community  
618 ordination and spatio-temporal monitoring. *Global Ecology and Biogeography*  
619 25:1144–1158.
- 620 Thorson, J. T., J. N. Ianelli, S. B. Munch, K. Ono, and P. D. Spencer. 2015. Spatial delay-  
621 difference models for estimating spatiotemporal variation in juvenile production and  
622 population abundance. *Canadian Journal of Fisheries and Aquatic Sciences* 72:1897–  
623 1915.
- 624 Thorson, J. T., J. E. Jannot, and K. Somers. In press. Using spatio-temporal models of  
625 population growth and movement to monitor overlap between human impacts and  
626 population density. *Journal of Applied Ecology*.
- 627 Thorson, J. T., H. J. Skaug, K. Kristensen, A. O. Shelton, E. J. Ward, J. H. Harms, and J. A.  
628 Benante. 2014. The importance of spatial models for estimating the strength of  
629 density dependence. *Ecology* 96:1202–1212.
- 630 Warton, D. I., F. G. Blanchet, R. B. O’Hara, O. Ovaskainen, S. Taskinen, S. C. Walker, and  
631 F. K. Hui. 2015. So Many Variables: Joint Modeling in Community Ecology. *Trends*  
632 *in Ecology & Evolution*.
- 633 Wootton, J. T., and M. Emmerson. 2005. Measurement of interaction strength in nature.  
634 *Annual Review of Ecology, Evolution, and Systematics*:419–444.

## 636 **Data Availability**

637 Data used in the case study were previously analyzed by Swain et al. (2015) and are publicly  
638 available at <http://dx.doi.org/10.5061/dryad.n43qf>. Statistical analysis used R package MIST  
639 v1.1.0 (<https://doi.org/10.5281/zenodo.260143>), and updated versions can be obtained via  
640 GitHub (<https://github.com/James-Thorson/MIST>).

641 Table 1 – Estimates and standard errors (in parentheses) for the interaction matrix ( $\mathbf{C} = \mathbf{B} +$   
 642  $\mathbf{I}$ ), where e.g. the 1<sup>st</sup> row and 2<sup>nd</sup> column represents the per-log-capita impact of white hake  
 643 and on per-capita productivity of Atlantic cod. This interaction matrix includes three  
 644 regulatory relations ( $R = 3$ ) amongst all four species (see Fig. 3).

|                     | <b>Atlantic cod</b> | <b>white hake</b> | <b>thorny skate</b> | <b>grey seal</b> |
|---------------------|---------------------|-------------------|---------------------|------------------|
| <b>Atlantic cod</b> | 0.860 (0.024)       | 0.095 (0.024)     | -0.031 (0.010)      | -0.060 (0.033)   |
| <b>white hake</b>   | -0.013 (0.007)      | 0.999 (0.008)     | 0.004 (0.003)       | -0.021 (0.015)   |
| <b>thorny skate</b> | 0.165 (0.048)       | 0.124 (0.045)     | 0.631 (0.060)       | -0.213 (0.078)   |
| <b>grey seal</b>    | -0.000 (0.002)      | -0.004 (0.003)    | 0.000 (0.001)       | 0.985 (0.005)    |

645  
 646 Fig. 1 Illustration of model selection results (top panel) using the Akaike Information  
 647 Criterion to select the number of regulatory relations  $R$  in the interaction matrix  $\mathbf{B}$  (the bold  
 648 number above each bar represents the proportion of simulation replicates where the model  
 649 did not converge), and boxplots illustrating root-mean-squared-error (RMSE) in estimates of

650 log-abundance for each species (bottom panel),  $\sqrt{(ST)^{-1} \sum_{t=1}^T \sum_{s=1}^S (x_{s,t,p} - \hat{x}_{s,t,p})^2}$ , where  
 651  $x_{s,t,p}$  is simulated and  $\hat{x}_{s,t,p}$  is predicted log-abundance for each model (the bold number  
 652 above each boxplot shows the average RMSE for all species and simulation replicates).

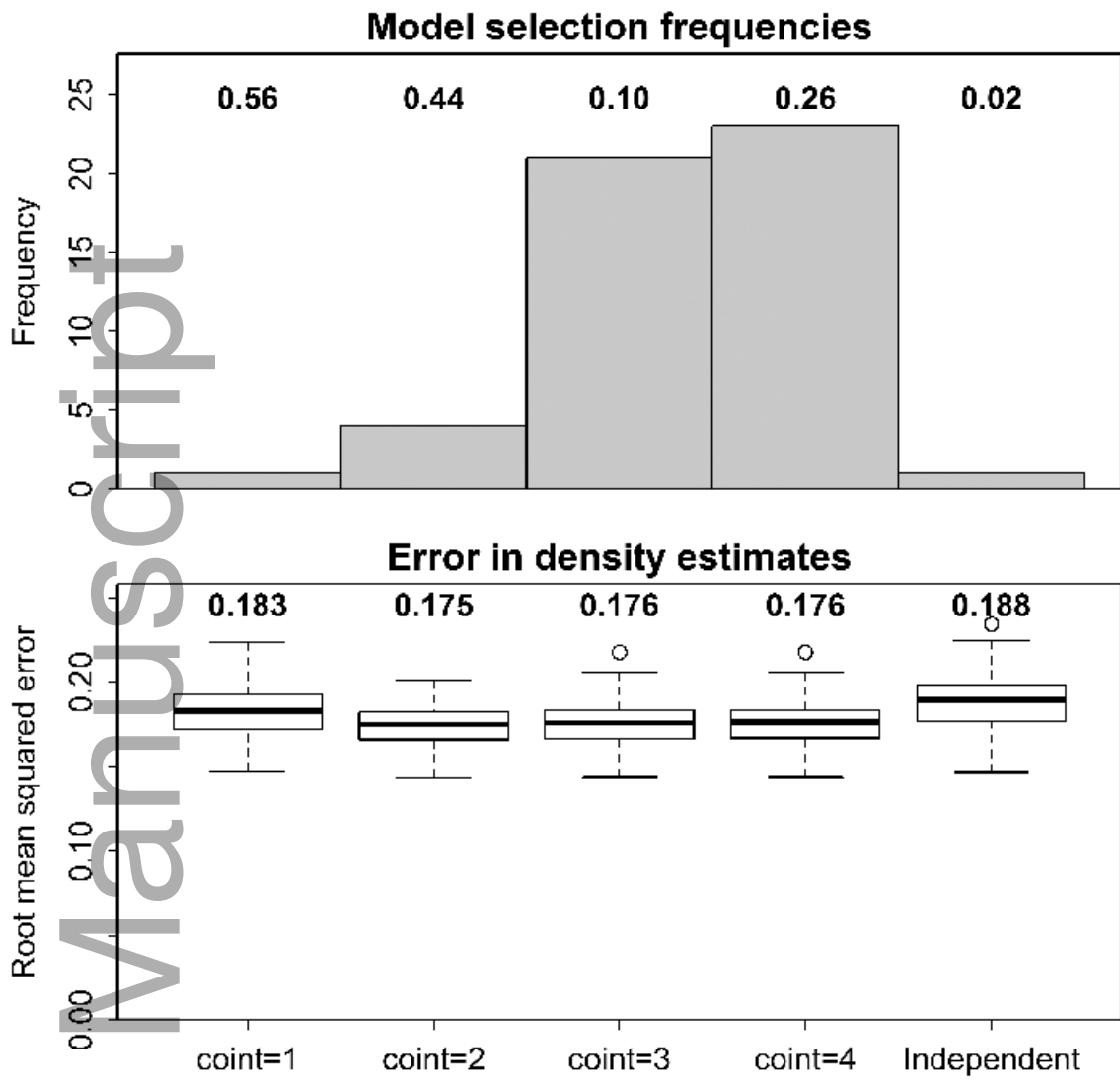
653 Fig. 2 – Illustration of estimated interaction matrix ( $\mathbf{C}=\mathbf{B}+\mathbf{I}$ ), where e.g., the top-left panel  
 654 shows the element  $c_{1,1}$  (note the different x-axis ranges for diagonal and off-diagonal  
 655 panels), and where the grey histogram represents the estimates from the estimated interaction  
 656 matrix  $\mathbf{C}$  from the model where  $R$  is selected using the Akaike Information Criterion, the red  
 657 histogram represents estimates from the model where  $\mathbf{B}$  is an estimated diagonal matrix (i.e.,  
 658 assuming single-species dynamics), and where the blue line is the true value (note the  
 659 different range in the x-axis for each panel).

660 Fig. 3 – Illustration of the eigen-decomposition of the interaction matrix ( $\mathbf{C}=\mathbf{B}+\mathbf{I}$ ) for our case  
 661 study. Each panel displays an eigenvalue (listed in the top), and displays values for the  
 662 column-eigenvector associated with that eigenvalue. An eigenvalue of 1.000 indicates a  
 663 dimension for community dynamics that follows a random-walk process.

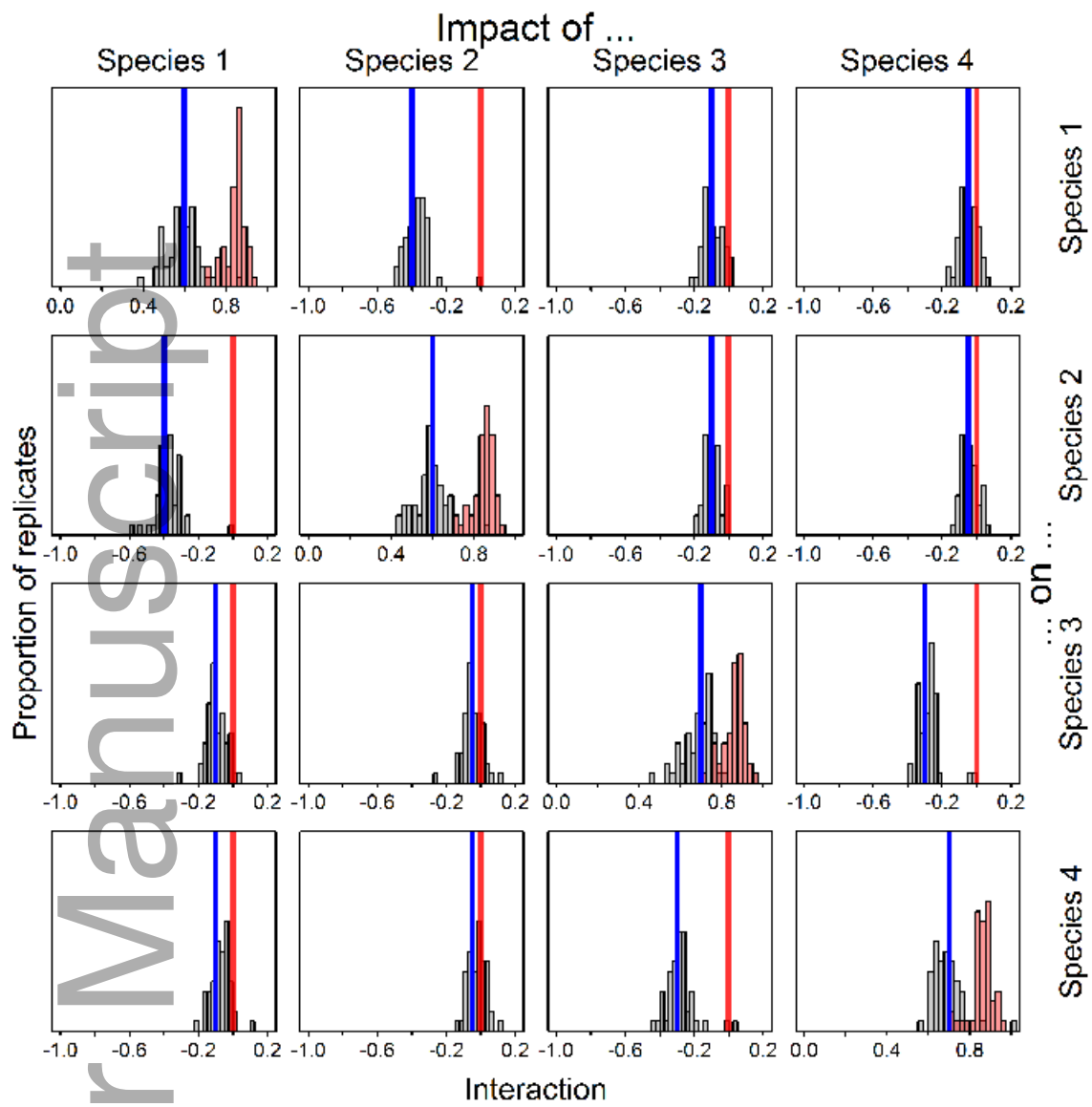
664 Fig. 4 – Illustration of estimated density  $\mathbf{X}_t$  for each of four species (columns) in the Gulf of  
 665 St. Lawrence for five evenly-spaced years (rows:  $t \in \{1971, 1981, 1992, 2002, 2012\}$ )  
 666 spanning the 42 year period with available data. Colors for each species represent density  
 667 relative to maximum (red) and minimum (blue) density observed for that species.

668 Fig. 5 – Estimated covariance of process errors ( $\Sigma_{\mathbf{E}}$ ) for the Gulf of St. Lawrence community  
669 dynamics case study (where we have assumed full-rank covariance, i.e.,  $K = P$ )

Author Manuscript

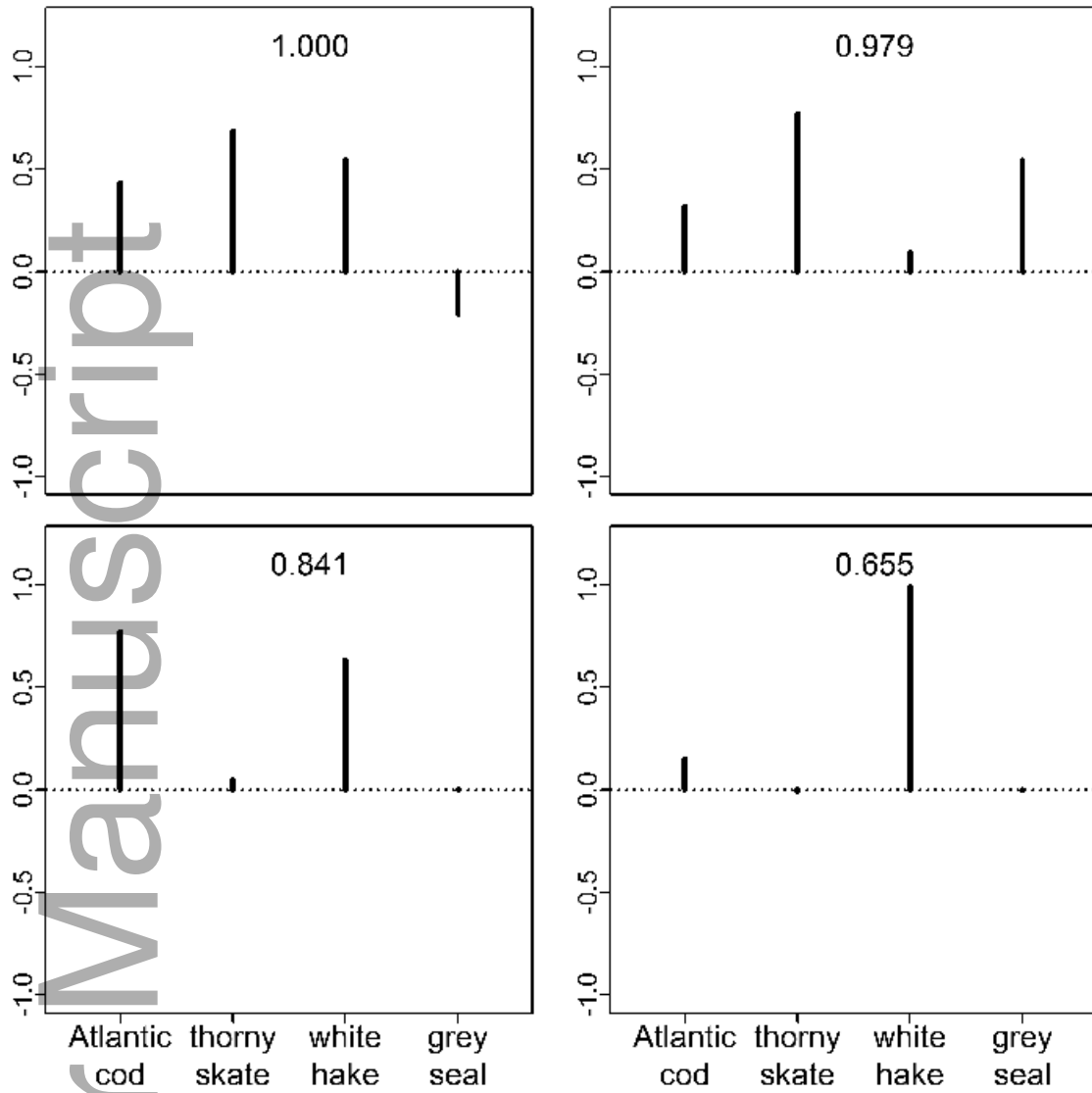


ecy\_1760\_f1.png

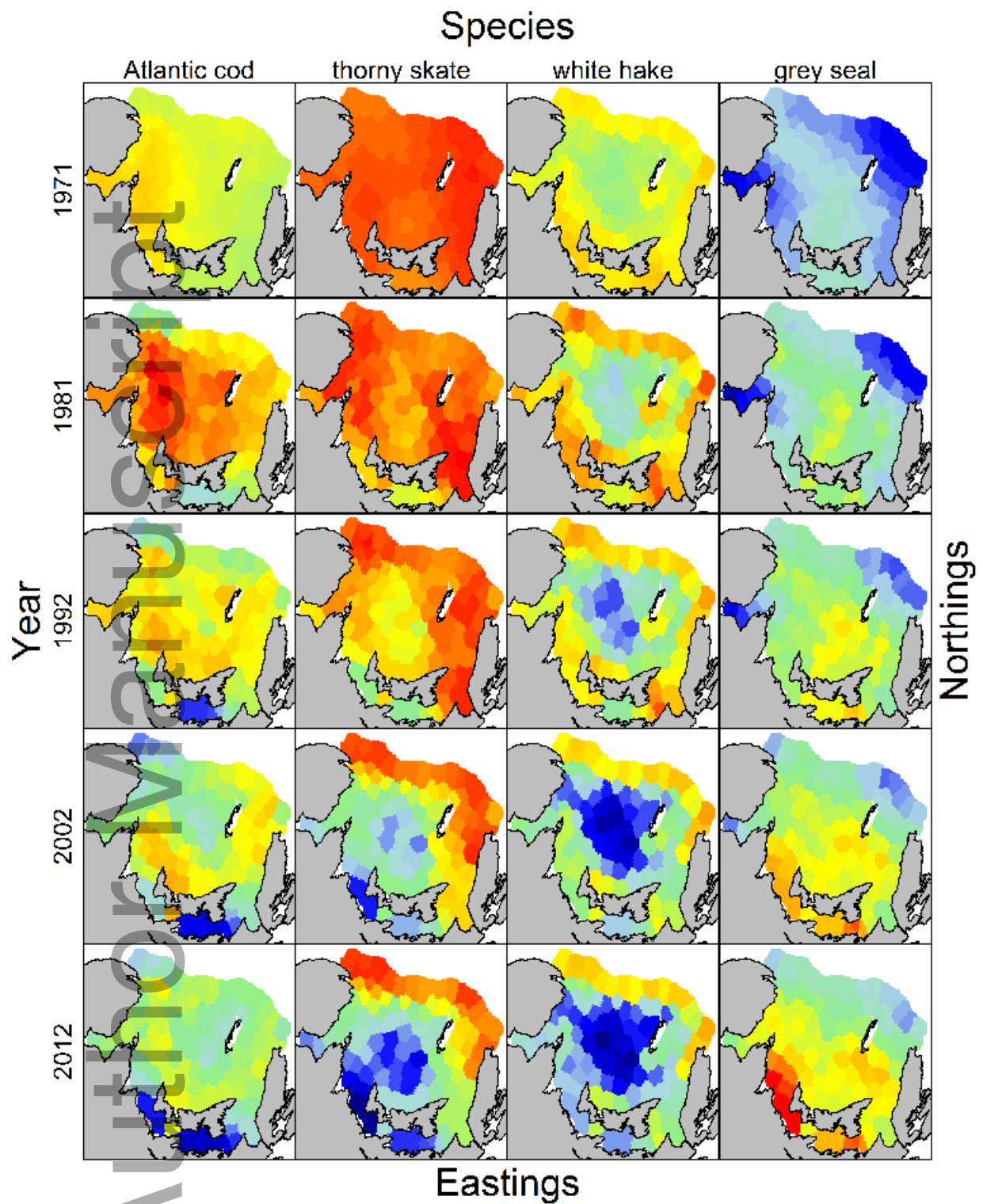


ecy\_1760\_f2.png

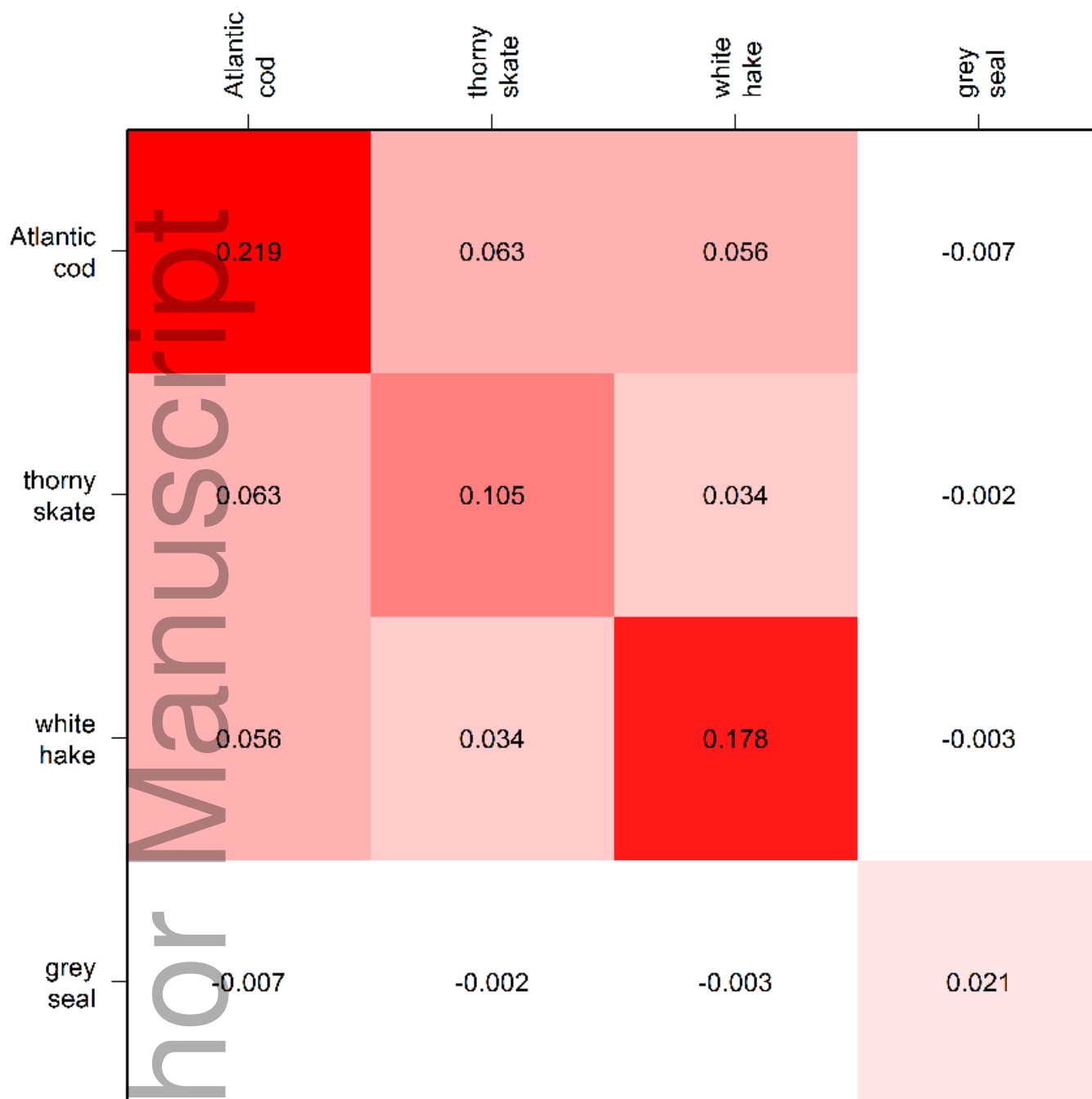




ecy\_1760\_f3.png



ecy\_1760\_f4.png



ecy\_1760\_f5.png